THE JOURNAL OF PHYSICAL CHEMISTRY C

Article

pubs.acs.org/JPCC

Effect of Electric Field on Condensed-Phase Molecular Systems. II. Stark Effect on the Hydroxyl Stretch Vibration of Ice

Sunghwan Shin,[†] Hani Kang,[†] Daeheum Cho,[‡] Jin Yong Lee,*[,‡] and Heon Kang*[,†]

[†]Department of Chemistry, Seoul National University, 1 Gwanak-ro, Seoul 151-747, South Korea

[‡]Department of Chemistry, Sungkyunkwan University, Suwon 440-746, South Korea

Supporting Information

ABSTRACT: We studied the Stark effect on the hydroxyl stretching vibration of water molecules in ice under the influence of an external electric field. Electric fields with strengths in the range from 6.4×10^7 to 2.3×10^8 V·m^{-1} were applied to an ice sample using the ice film capacitor method. Reflection absorption infrared spectroscopy was used to monitor the field-induced spectral changes of vibrationally decoupled O−H and O−D bands of dilute HOD in D_2O and H_2O−ice, respectively. The spectral changes of the hydroxyl bands under applied field were analyzed using a model that simulates the absorption of a collection of Stark-shifted oscillators. The analysis shows that the Stark tuning rate of ν(O−D) is 6.4−12 cm^{-1}/(MV·cm^{-1}) at a field strength from 1.8×10^8 to 6.4×10^7 V·m^{-1}, and the Stark tuning rate of ν(O−H) is 10−16 cm^{-1}/(MV·cm^{-1}) at a field strength from 2.3×10^8 to 9.2×10^7 V·m^{-1}. These values are uniquely large compared to the Stark tuning rates of carbonyl or nitrile vibrations in other frozen molecular solids. Quantum mechanical calculations for the vibrations of isolated water and water clusters show that the vibrational Stark effect increases with the formation of intermolecular hydrogen bonds. This suggests that that the large Stark tuning rate of ice is due to its hydrogen-bonding network, which increases anharmonicity of the potential curve along the O−H bond and the ability to shift the electron density under applied electric field.

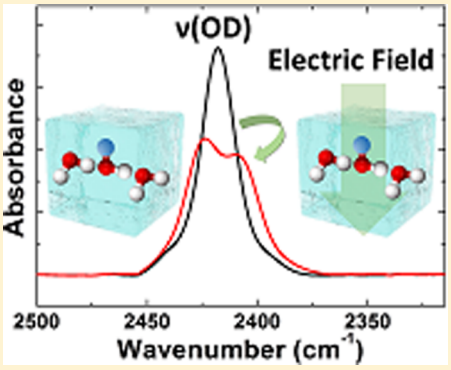

1. INTRODUCTION

Electric fields can shift the absorption frequencies of molecular vibrations by changing the dipole moment and polarizability of molecules associated with the vibrational transitions.[1,2] This phenomenon, known as the vibrational Stark effect (VSE), is an important aspect of IR spectroscopy in condensed phases. Inhomogeneous broadening of the condensed-phase IR spectra is produced largely by the Stark shift of vibrational frequencies under the influence of local fields in the solvent.[3,4] Experimental investigations of the VSE require the application of strong electric fields (>10^7 V·m^{-1}), so that the effects of the applied field can be detected over the inherent spectral broadening due to the local fields. The application of a strong external field, however, causes several practical problems such as dipolar polarization and dielectric breakdown of the sample. To circumvent these limitations, Boxer and co-workers[1] have developed a method to immobilize the chromophore molecules in a glassy sample and apply the electric field across the sample using electrically biased metal electrodes. This method has been successfully applied for measuring the Stark tuning rates ($\Delta\mu$) of various chromophore groups in frozen molecular solids, and the information acquired from these measurements has been used to probe internal electric fields in biological molecular systems.[2,5]

The hydroxyl stretching vibration of water is a key spectroscopic feature in the study of water structure and dynamics, including intermolecular hydrogen bonding, solute−solvent interactions, vibration dynamics, and interfacial water geometry.[3,4,6−9] These subjects have been actively studied in recent years. However, despite its importance, the Stark tuning rate of the hydroxyl stretch vibration of liquid or solid water has not been precisely determined from spectroscopic experiments so far. Theoretical methods have been mostly used to compute the Stark tuning rate and spectral shift under local fields in solvents, and the resultant inhomogeneous line broadening has been compared with the experimentally observed line shapes of the hydroxyl stretch vibrations.[3,4,6−8]

Investigation of the VSE of hydroxyl stretch vibration poses additional difficulties due to the inherent complexity of the IR spectra of water in a condensed phase. For example, the IR spectrum of ice is complicated by contributions from several competing factors.[10] The hydroxyl stretching frequency is sensitive to the local environment of ice because the local field varies with the proton-disordered arrangement of the lattice. In addition to the intramolecular vibrational couplings of isolated water molecules, intermolecular vibrational couplings and couplings to lattice vibrations tend to delocalize the vibrational modes. To separate these vibrational coupling effects, samples containing dilute HOD in either D_2O or H_2O−ice have been used in many experiments.[11−15] In these systems, the

Received: February 25, 2015
Revised: May 15, 2015
Published: May 19, 2015

DOI: 10.1021/acs.jpcc.5b01850
J. Phys. Chem. C 2015, 119, 15596−15603

vibrational coupling effects are negligible for the O−H (or O−D) stretch of HOD, and the experimental O−H (or O−D) line shapes can directly reflect the effect of the local electric field. Therefore, we have chosen to use these systems for studying the VSE for the hydroxyl stretch vibration in ice. The ice film capacitor method has been used to apply strong electric fields to the samples.[16] This paper is the second of a series of two papers (referred to as Paper I[17] and Paper II) investigating the effects of electric field on frozen molecular films.

2. EXPERIMENTAL METHODS

The apparatus, electric field generation method, and spectroscopic techniques have been described in detail in Paper I.[17] Therefore, the experimental methods are only briefly described in this paper.

Ice samples containing vibrationally decoupled HDO were prepared as follows. An H_2O film was grown by condensing H_2O vapor on a Pt(111) single crystal surface at a deposition rate less than 0.1 ML·s^{-1} (where one monolayer (ML) = 1.1× 10^{15} water molecules·per square centimeter) using a backfilling method. Over this film, which is used as a spacer layer, another H_2O film containing dilute HDO was deposited by condensing the vapor of an H_2O−HDO mixed solution through a tube doser at a deposition rate <0.1 ML·s^{-1}. The H_2O−HDO mixture with a low (e.g., ∼7%) HDO concentration was prepared by mixing liquid H_2O and D_2O in a 96.5:3.5 ratio at room temperature, where most of the D_2O was converted into HDO through entropic H/D exchange. The isotopolog composition of the vapor was verified using a quadrupole mass spectrometer installed in the chamber. The ice films were grown at a Pt substrate temperature of 140 K and then heated at 150 K for 100 s to ensure the formation of a crystalline ice phase.[18] A D_2O sample containing dilute HDO was prepared using the same procedure as above, except that D_2O was used instead of H_2O.

Electric field was applied across the ice samples using the ice film capacitor method,[16] in which the ice film surface was charged positively with Cs^+ ions and the Pt substrate surface was charged negatively with electrons. The sample temperature was maintained at 70 K during the deposition of Cs^+ ions and subsequent spectroscopic measurements. The electric field strength (F) inside the ice film can be calculated from the relationship $F = V/d = \sigma/\varepsilon_r\varepsilon_0$, where V is the voltage across the film, d is the film thickness, σ is the surface density of Cs^+ ions, ε_r is the relative permittivity of the film, and ε_0 is the vacuum permittivity. The voltage across the film was measured using a Kelvin probe, and the film thickness was estimated from temperature-programmed desorption (TPD) measurements. The effects of applied electric field on the sample were investigated with reflection absorption infrared spectroscopy (RAIRS). Differences in the RAIR spectra measured in the presence and absence of electric field represented the change in the absorbance (ΔA) of the sample induced by the applied field.

3. RESULTS

3-A. RAIR Spectrum of the Hydroxyl Stretch Band. Figure 1 shows the RAIR spectra obtained from a crystalline ice sample consisting of ∼7% HDO and ∼93% H_2O. The absorbance spectrum measured in the absence of an external electric field is shown at the top. The spectrum shows a small peak at ∼2420 cm^{-1}, which corresponds to the ν(O−D) stretching vibration of HDO molecules diluted in ice. The nearly symmetric Gaussian shape of this peak indicates that the ν(O−D) vibrational band is comprised of a single oscillator component, which is decoupled from the other water vibrations. A large ν(O−H) stretching band attributed to H_2O−ice appears at 3000−3500 cm^{-1}, with the characteristic spectral shape of ice Ih crystals.[18]

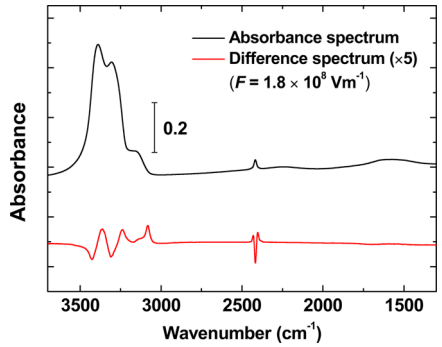

Figure 1. (upper) RAIR spectrum of crystalline ice composed of ∼7% HDO and ∼93% H_2O measured in the absence of an external electric field. (lower) The field-on minus field-off difference spectrum, which corresponds to the absorbance difference (ΔA) of a sample in the presence and absence of applied field. The field strength was 1.8 × 10^8 V·m^{-1}. The difference spectrum is displayed on a magnified scale (×5).

Application of an external electric field with a strength of 1.8 × 10^8 V·m^{-1} changed the shapes of the ν(O−H) and ν(O−D) bands significantly. The changes are apparent in the field-on minus field-off difference spectrum displayed at the bottom of Figure 1. The ν(O−D) band in the difference spectrum shows a dip at the peak center and an increased absorbance at the peak edges. These changes indicate that the ν(O−D) bandwidth is broadened by the field. The ν(O−H) spectrum of H_2O shows more complex changes under applied field. The shape of this band is a result of many factors including intermolecular vibrational couplings in ice, which are not fully identified yet.[10] For this reason, we will not discuss the changes in this band in the present paper. We will focus only on the ν(O−D) and ν(O−H) bands of vibrationally decoupled HOD.

Figure 2a shows the magnified spectra of the ν(O−D) band of dilute HDO in H_2O−ice measured at increasing field strengths. Spectral broadening of the band under applied field is clearly evident. The full width at half-maximum (fwhm) of the band, which is ∼20 cm^{-1} at zero field, increases to ∼37 cm^{-1} at 1.8 × 10^8 V·m^{-1}. In addition, the sharp protrusion at the center seen at zero field becomes increasingly flat and even transforms into a dip at the highest applied field strength (1.8 × 10^8 V·m^{-1}). Further, the symmetric Gaussian shape of the ν(O−D) band becomes slightly asymmetric under applied field, with higher absorbance observed on the high frequency side. These changes are clearly visible in the difference spectra as well. The spectral broadening indicates the appearance of the Stark effect. The Stark effect appears as a spectral broadening rather than a shift in peak position because the chromophores are randomly oriented in the sample.

Figure 2b shows the results for the ν(O−H) band (∼3270 cm^{-1}) of diluted HDO in the D_2O−ice crystal. The evolution of the spectral shape with increasing field strength is very similar to the behavior observed for ν(O−D) in Figure 2a. Owing to the close resemblance of the two systems in

DOI: 10.1021/acs.jpcc.5b01850
J. Phys. Chem. C 2015, 119, 15596−15603

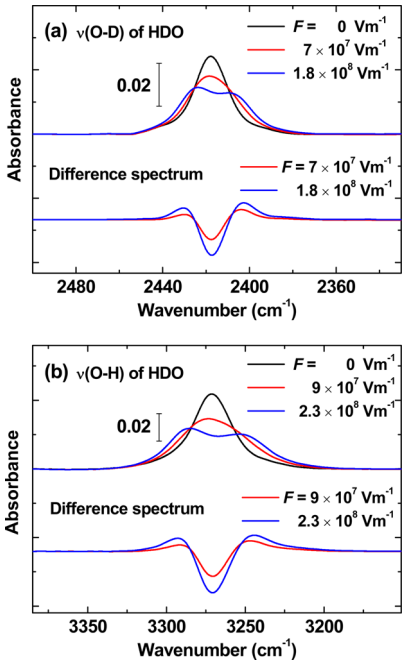

Figure 2. (a) (upper) RAIR spectra showing spectral broadening of the ν(O−D) band of dilute HDO in H_2O−ice with increasing applied electric field. (lower) The field-on minus field-off difference spectra for the absorbance spectra shown at the top. (b) Spectral broadening of the ν(O−H) band of dilute HDO in D_2O−ice. The relative population of HDO in ice was ∼7% in both the samples.

qualitative features, only one of these results will be shown as representative behavior in the rest of the paper.

In the present work, we chose to use a crystalline ice sample for studying the VSE, instead of an amorphous solid water (ASW) sample, for the following reasons. First, crystalline ice exhibits narrower inhomogeneous band broadening compared to ASW (fwhm of the ν(O−D) band of ASW is ∼69 cm^{-1}). A narrow band is obviously advantageous in detecting the additional spectral broadening due to applied electric field, which is observed to be ∼17 cm^{-1} at an applied field strength of 1.8 × 10^8 V·m^{-1}. Second, the use of a crystalline sample prohibits the reorientation of water molecules in the lattice at low temperatures under applied field, which will be shown shortly after. On the other hand, ASW has a more floppy lattice structure, and reorientation of water molecules may occur under applied field, which may cause additional spectral changes. Therefore, the experiment with a crystalline ice sample measures the VSE of the hydroxyl stretch band produced only by applied electric field (electrostatic effect), eliminating other frequency shifting effects (structural and chemical effects) coming from changes of the chromophore environment under the electric field.[19−21] The field-induced reorientation of molecules is investigated for amorphous solid acetone samples in Paper I.

We examined the change in the ν(O−D) band shape as the field strength was progressively increased and decreased. To increase the field strength, Cs^+ ions were added on the ice film surface via ion beam deposition, whereas to decrease the field strength, low-energy (∼10 eV) electrons were sprayed onto the sample surface.[17,22] Since the sample surface was positively charged after the initial Cs^+ deposition, it easily attracted low-energy electrons to neutralize the surface charge. The field strength was estimated using the Kelvin probe measurements after each charging (Cs^+ deposition) or discharging (electron deposition) step. Figure 3 shows the variation in the ν(O−D)

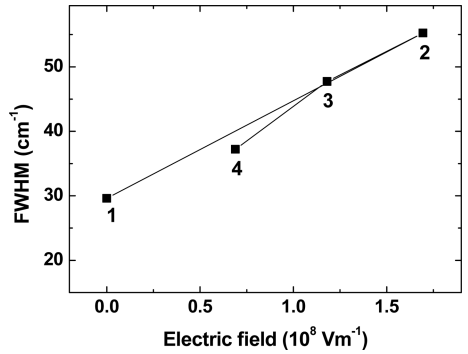

Figure 3. Variation in the spectral width (fwhm) of ν(O−D) as the electric field strength was increased and decreased. The numbers within the plot indicate the field change sequence.

bandwidth measured as the electric field strength was changed. The sample contained ∼5% HDO in H_2O−ice. Owing to the lower HDO content in this sample compared to the ones used for the results shown in Figure 2, the observed bandwidth is slightly larger; this is due to large spectral noises of the weak signal. Figure 3 shows that the ν(O−D) bandwidth changes almost reversibly with change in the field strength. The reversible behavior indicates that the changes are due to an electronic effect, and therefore VSE, rather than being a result of structural change in the sample.

3-B. Stark Tuning Rate. We performed spectral analysis to analyze the changing profile of the hydroxyl bands under applied field and estimate the extent of Stark shift. Andrews and Boxer[23] have developed an analytical model to analyze the Stark difference spectra based on the second derivative of absorbance spectra. This model has been successfully applied for studying the VSE at field strengths below 1 × 10^8 V·m^{-1}.[1,2] Figure 4a shows the experimental Stark difference spectrum of ν(O−D) band measured at a field strength of 1.8 × 10^8 V·m^{-1}, together with the simulated second-derivative spectrum fitted to the experimental spectrum. The fitting result is not satisfactory, with a significant mismatch in the peak positions between the experimental and simulated spectra. We believe that the discrepancy is mainly caused by the strong external field used in the present study and a large Stark shift of the hydroxyl stretch frequency. Therefore, we undertook an approach to directly simulate the absorbance spectrum, rather than the difference spectrum, using a numerical analysis method, which is described below.

According to the theory of VSE, the peak shift ($\Delta\nu$) of individual oscillators under the influence of electric fields can be expressed by eq 1.[2]

$$\Delta\nu \cong -\frac{1}{h}\left(\Delta\mu\cdot\mathbf{F} + \frac{\mathbf{1}}{\mathbf{2}}\mathbf{F}\cdot\Delta\alpha\cdot\mathbf{F}\right) \quad (1)$$

eq where $\Delta\mu$, the Stark tuning rate, represents the difference in dipole moments between the ground and excited states, expressed typically in units of $cm^{-1}/(MV/cm^{-1})$ or in Debye, F is the electric field, and $\Delta\alpha$ is the difference in polarizabilities. Equation 1 is an approximate formula including only the first- and second-order terms for F in the series expansion.

The hydroxyl stretching vibration spectrum in the presence of an external field is simulated by considering the Stark shift of

DOI: 10.1021/acs.jpcc.5b01850
J. Phys. Chem. C 2015, 119, 15596−15603

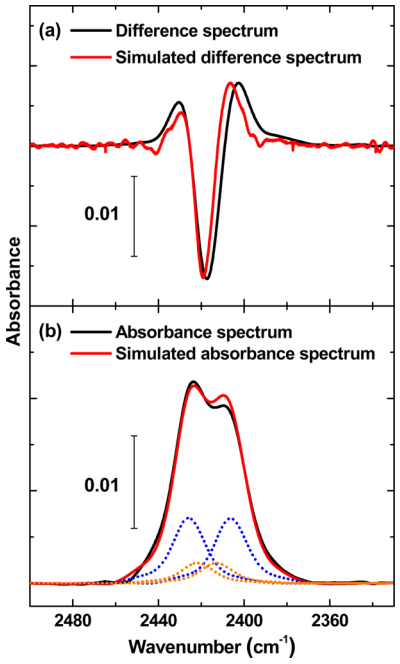

Figure 4. Spectral analysis of the ν(O−D) band of dilute HDO in H_2O−ice using different models. The applied field strength is 1.8 × 10^8 V·m^{-1}. (a) The experimental difference spectrum (black) is fitted to the model developed by Andrews and Boxer (red).[23] (b) The experimental absorbance spectrum (black) is fitted to the results of the numerical simulations (red). The dotted curves represent the simulated absorbance for O−D oscillators with the polar angle with respect to the field direction between θ = 30° ± 10° (blue), θ = 70° ± 10° (orange), θ = 110° ± 10° (orange), and θ = 150° ± 10° (blue). These curves illustrate that the oscillators in the near-polar angles (blue) contribute a larger amount of absorbance to the spectrum than those in the near-equatorial angles (orange) due to the $\cos^2(\theta)$ factor (see text), although the number of oscillators in the near-polar solid angle is smaller than that in the near-equatorial solid angle.

individual oscillators under F using eq 1. In this approach, we first simulate the Stark-shifted absorbance signal of an O−D oscillator in the RAIRS experimental geometry as follows. The absorbance (A) of an oscillator varies with the angle (θ) between the transition dipole moment of an oscillator and the direction of p-polarized light according to the relationship $A \propto \cos^2(\theta)$.[17,24] In addition, the amount of Stark frequency shift of an oscillator is proportional to the cosine of the angle (γ) between the applied electric field and the transition dipole moment, as shown in eq 1. In the present RAIRS geometry, θ and γ are equal.

Subsequently, the simulated absorption intensities of a total of 8 × 10^5 oscillators are summed over their isotropic angular distribution. The resulting absorption spectrum is the $\cos^2(\theta)$ weighted average of a collection of Stark-shifted absorption peaks. The simulation procedure is described in more detail in the Supporting Information. Figure 4b shows the simulated ν(O−D) absorption spectrum overlapped with the experimental absorbance spectrum. The simulated curve is fitted to the experimental curve by adjusting the $|\Delta\mu|$ and $|\Delta\alpha|$ values of eq 1. According to the simulation results of the spectral fitting, $\Delta\mu$ plays a dominant role in spectral broadening at the field strength used in the present study, whereas the contribution of the $\Delta\alpha$ term to spectral broadening is minor. Nevertheless, it is necessary to include the $\Delta\alpha$ term to reproduce the asymmetry in the ν(O−D) spectral shape appearing under the field. A comparison of the curve-fitting results shown in Figure 4a,b indicates that the numerical analysis method simulates the spectral changes more accurately than the second derivative analysis method.

The value of $\Delta\mu$ can be deduced by optimizing the spectral fitting to the experimental data as shown in Figure 4b. The estimated $\Delta\mu$ values are 12 cm^{-1}/(MV·cm^{-1}) (or 0.70 D) and 6.4 cm^{-1}/(MV·cm^{-1}) at field strengths of 6.4 × 10^7 V·m^{-1} and 1.8 × 10^8 V·m^{-1}, respectively. Likewise, the $\Delta\mu$ values for ν(O−H) of vibrationally isolated HDO in D_2O−ice are estimated to be 16 cm^{-1}/(MV·cm^{-1}) and 10 cm^{-1}/(MV·cm^{-1}) at field strengths of 9.2 × 10^7 V·m^{-1} and 2.3 × 10^8 V·m^{-1}, respectively. The $\Delta\mu$ values for ν(O−H) and ν(O−D) obtained at field strengths in the range from 6.4 × 10^7 to 2.3 × 10^8 V·m^{-1} are plotted in Figure 5. It was difficult to deduce the $\Delta\alpha$ value with reliable accuracy with this procedure because $\Delta\alpha$ has a relatively minor influence on the spectral change.

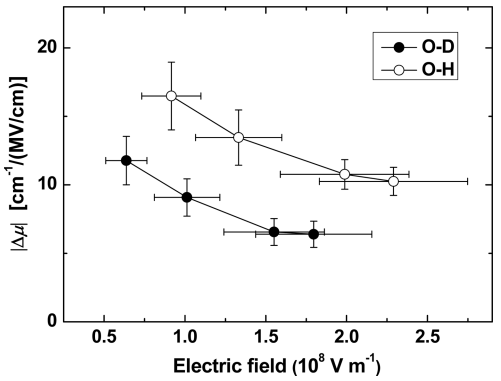

Figure 5. Stark tuning rates of the ν(O−H) and ν(O−D) bands of ice measured at different field strengths.

A few observations may be made regarding the Stark tuning rates presented in Figure 5. First, the $\Delta\mu$ value of the hydroxyl stretching vibration of ice is over 10 times larger than that of typical chromophore groups of other frozen molecular solids, including $\Delta\mu$(C≡N of acetonitrile), which is 0.23−0.6 cm^{-1}/(MV·cm^{-1}),[16,23] and $\Delta\mu$(C≡O), which is 0.67 cm^{-1}/(MV·cm^{-1}).[23,25] Second, the $\Delta\mu$ value of ν(O−H) is 1.5−1.8 times larger than that of ν(O−D) at the same field strength. Third, the $\Delta\mu$ values decrease with increasing field. In eq 1, it is assumed that $\Delta\mu$ is a constant for linear proportionality between $\Delta\nu$ and F. According to the present results, however, $\Delta\nu$ varies quite nonlinearly with F. As mentioned above, the second-order ($\Delta\alpha F^2$) term has only minor influence on spectral broadening. For instance, when we double the $\Delta\alpha$ value in the numerical simulation and make the spectral fitting, this change alters the estimated value of $\Delta\mu$ by less than 15%. This indicates that the observed variation in $\Delta\mu$ with electric field strength is unlikely to be due to the second and higher order terms for F. Under such circumstances, it seems necessary to consider $\Delta\mu$ as a field-dependent parameter when eq 1 is used to express the Stark frequency shift observed over a wide field range.

4. THEORETICAL STUDY

4-A. Computational Details. We simulated the VSE of water molecules in ice for three model systems, namely, water monomer (HDO; **w1**), dimer [$(HDO)_2$; **w2**], and octamer [$(HDO)_8$; **w8**]. In the first model (**w1**), the VSE of a single

DOI: 10.1021/acs.jpcc.5b01850
J. Phys. Chem. C 2015, 119, 15596−15603

water molecule was investigated, whereas in the dimer model (**w2**), the effect of intermolecular hydrogen bonding on the Stark shift was examined. The octamer model (**w8**), which includes **w2** and its first hydration shell (six water molecules), was used to investigate the effect of the coordinating water molecules on the Stark shift. The calculated equilibrium geometries of the water clusters are shown in Figure 6. The

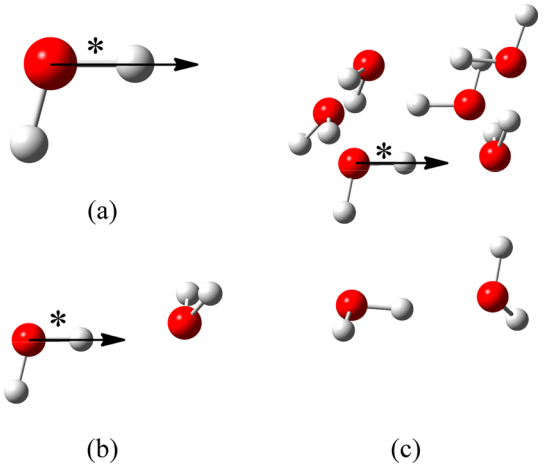

Figure 6. Optimized geometries of (a) **w1**, (b) **w2**, and (c) **w8** without an external electric field. The direction of external field (arrow) is drawn on the O−D bonds of interest (marked with a star).

external electric field was applied along the O → D bond direction (indicated by an arrow in the figure) of water clusters. A potential energy surface scan was performed for the O−D stretch in **w1**, **w2**, and **w8** under an external electric field using the second-order Møller−Plesset perturbation (MP2)[26,27] level of theory with the augmented correlation-consistent polarized valence double-ζ (aug-cc-pVDZ) basis set. The potential energy curves obtained were then fitted to Morse potentials of the form $V(r) = D(1-e^{-\alpha(r-r_e)})^2$, where D is the bond dissociation energy, α is a width-related parameter, and r and r_e are the O−D distance and its equilibrium value, respectively. The vibrational energy levels in the Morse oscillator, E_n, are given by $E_n = DB(n + (1/2))[2 - B(n + (1/2))]$, where n is the vibrational quantum number, and $B^2 = (\alpha^2\hbar^2/2\mu D)$, where μ is the reduced mass of the molecular species of interest. All the calculations were performed with the Gaussian09 program.[28]

4-B. Computational Results. The potential energy curves for the O−D bond of **w1**, **w2**, and **w8** under an external electric field are plotted in Figure 7. The solid circle in the figure represents the ab initio potential energy surface scan of **w1**, **w2**, and **w8** as a function of the O−D bond stretch distance (−0.16 Å < $r - r_{eq}$ < 0.24 Å at intervals of 0.04 Å). The data were then fitted to the Morse potentials of solid lines. The ground and first excited vibrational states were also indicated by horizontal solid lines. The vibrational transition frequency of **w1** in the absence of an external field (2738 cm^{-1}) matches well with previous experimental (2724 cm^{-1})[29] and theoretical results (2775 cm^{-1}).[3] The $\Delta\mu$ deduced from the Morse potential fit analyses are listed in Table 1, along with the experimental

Table 1. Comparison of the Theoretical and Experimental Stark Tuning Rates ($\Delta\mu$ in $cm^{-1}/(MV{\cdot}cm^{-1})$) for the O−D Stretch Vibration of HOD

theoretical (water cluster)	**w1**	**w2**	**w8**
	0.35	0.69	4.8
experimental (ice)	6.4 ($F = 1.8 \times 10^8$ V·m^{-1}) − 12 ($F = 6.4 \times 10^7$ V·m^{-1})		

values estimated in Section 3-B. The effect of internal electric field on the computed $\Delta\mu$ value was considered. For this, we calculated internal field (F_{int}) and its change (ΔF_{int}) under the influence of external electric field (F_{ext}). ΔF_{int} is responsible for the Stark broadening and thus the computed Stark tuning rate. The internal field strength is highly dependent on the reference point at which the electric field is calculated due to the influence of surrounding molecules. In our calculation, the middle point of O−D bond was used as a reference point. Although the internal field was stronger than the applied external field ($|F_{int}| > |F_{ext}|$), the change in the internal field was smaller than the external field ($|\Delta F_{int}| < |F_{ext}|$). ΔF_{int} was typically ∼1/7 of F_{ext}. This indicates that the internal field has only minor influence on the computed Stark tuning rate.

The $\Delta\mu$ value of **w1** is very small [0.35 $cm^{-1}/(MV{\cdot}cm^{-1})$], suggesting that the experimental $\Delta\mu$ of ice cannot be predicted by considering the properties of single molecules alone. At first glance of Figure 7, the change in the potential energy curve of **w1** with respect to external field appears to be almost negligible. However, **w2** exhibits a greater VSE than **w1**, with noticeable difference in the potential energy curve as a function of external field. The $\Delta\mu$ value of **w2** is 0.69 $cm^{-1}/(MV/cm)$, about twice that of **w1**. The dimer geometry can provide at least a partial explanation for the experimental observation. The increase in $\Delta\mu$ observed for **w2** compared to **w1** is likely to be caused by intermolecular hydrogen bonding. The hydrogen bridge between the water monomers allows facile transfer of electrons from one monomer to the other. Hence, the potential energy curve for O−D of **w2** is more prone to vary with external field compared to that of **w1**, resulting in a larger $\Delta\mu$.

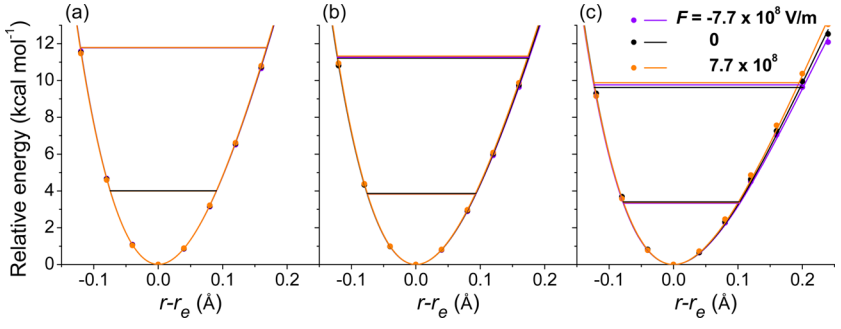

Figure 7. Potential energy curve for O−D in (a) **w1**, (b) **w2**, and (c) **w8** at applied field strengths of -7.7×10^8, 0, and 7.7×10^8 V·m^{-1}.

DOI: 10.1021/acs.jpcc.5b01850
J. Phys. Chem. C 2015, 119, 15596−15603

In the octamer model (**w8**), $\Delta\mu$ drastically increased to 4.8 $cm^{-1}/(MV/cm)$ on average at $F = -7.7 \times 10^8$ and 7.7×10^8 $V \cdot m^{-1}$. This value is close to the experimental value of 6.4 $cm^{-1}/(MV \cdot cm^{-1})$ measured at a field strength of 1.8×10^8 $V \cdot m^{-1}$. Although we applied the external field along O−D bond to investigate the vibrational Stark effect because many previous studies focused on the frequency changes with respect to the local electric field along the O−D bond axis, the angle between the applied field and O−D bond may vary. When the external field was applied perpendicular to the O−D bond direction, the $|\Delta\mu|$ value of **w8** was calculated to be very small [0.4−0.8 $cm^{-1}/(MV/cm)$ depending on the azimuthal angle]. Therefore, if various field orientations were considered, the ensemble-averaged $\Delta\mu$ value would be smaller than 4.8 $cm^{-1}/(MV/cm)$. Consistent with the observed trend for different cluster sizes, the first excited vibrational state of **w8** shows the most significant change under applied field among **w1**, **w2**, and **w8**, which is attributed to the greatest change in the potential energy curve of **w8** among the three (Figure 7c). We believe that the drastic increase in $\Delta\mu$ observed for **w8** results from greater anharmonicity generated by coordinating water molecules.

To understand the greater anharmonicity for the potential energy curves of **w8**, it is necessary to explore the effect of the internal electric field generated by the Coulombic interactions between water molecules. For this purpose, the potential energy curves in Figure 7 have been rearranged to allow comparison of the curves from **w1**, **w2**, and **w8** at the same field strength, as shown in Figure 8. This comparison illustrates that

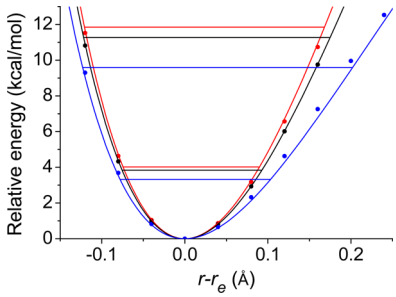

Figure 8. Comparison of the potential energy curves of O−D for **w1** (red), **w2** (black), and **w8** (blue) without an external field.

the intermolecular hydrogen bonding causes significantly larger changes in the potential energy curves compared to the changes caused by the external field in Figure 7. Two features can be noticed from Figure 8. The energy of the potential energy curve is lowered for **w2** and **w8** compared to **w1**, and the anharmonicity of the O−D vibration is substantially increased in **w8**. Both of these phenomena stem from the fact that the presence of a larger number of neighboring water molecules can better stabilize the stretched O−D bond via the hydrogen bond network inside the water cluster. The enhanced anharmonicity of the O−D oscillator possibly induces greater changes in the difference of the dipole moments and polarizabilities.

5. DISCUSSION

The experimental measurements in the present study show that the hydroxyl stretch vibration of ice exhibits a uniquely large Stark effect. The $\Delta\mu$ of this vibrational mode is over 10 times larger than those of carbonyl[23,25] and nitrile groups[16,23] of frozen molecular solids. Quantum mechanical calculations show that the value of $\Delta\mu$ increases from the water monomer to the dimer to the octamer as a result of the formation of intermolecular hydrogen bonds among the water molecules. The intermolecular hydrogen bonding increases the anharmonicity of the potential energy curve of the hydroxyl bond as well as the polarizability of the system to shift the electron density. This study suggests that the large $\Delta\mu$ value of ice is due to the extended hydrogen-bonding network of the lattice, which does not exist for many other frozen solvents. By the same token, it is expected that liquid water also exhibits a large VSE, owing to its extended hydrogen-bonded structure.

Although the theoretical study offers qualitative explanations for the origin of the increased VSE in ice, a gap still appears to exist between the experimental and computed $\Delta\mu$ values. The theoretical value of $\Delta\mu$ for **w8** (4.8 $cm^{-1}/(MV \cdot cm^{-1})$) is closest to the experimental value measured at high field strength (6.4 $cm^{-1}/(MV \cdot cm^{-1})$ at 1.8×10^8 $V \cdot m^{-1}$), and the two results may be considered to be in reasonable agreement in view of the simplicity of the water cluster model. Yet, the theoretical value is substantially lower than the experimental measurement at low field strength (12 $cm^{-1}/(MV \cdot cm^{-1})$ at 6.4×10^7 $V \cdot m^{-1}$). Skinner and co-workers[3] reported the values of $\Delta\mu$(O−D) = 1.6 $cm^{-1}/(MV \cdot cm^{-1})$ and $\Delta\mu$(O−H) = 2.4 $cm^{-1}/(MV \cdot cm^{-1})$ from liquid water simulations, which are also substantially lower than the experimental values. Interestingly, however, as far as the H/D isotopic effect is concerned, the theoretical[3] and experimental Stark tuning rates agree with each other with the $\Delta\mu$(O−H)/$\Delta\mu$(O−D) ratio in the range of 1.5−1.8.

The difference between the experimental and computed $\Delta\mu$ values draws our attention to the issue of local field correction, which is an idea that the local field near a chromophore, which is contributed by solvent molecules, may also change with the applied field.[2] The local field change can be incorporated into the present spectral analysis procedure, described in Section 3-B, by including an additional field term (F_{local}) that varies with the externally applied field (F_{ext}). In other words, $F = F_{ext} + F_{local}$ can be used in the place of electric field in eq 1. However, spectral fitting with the present model is quite satisfactory even without incorporating F_{local}, as shown in Figure 4, and the fitting quality is hardly improved by including an additional electric field term. Therefore, the local field correction effect must be small for the present case. This conclusion deduced from the experimental spectral fitting agrees with the theoretical calculation results that the internal field change (ΔF_{int}) is ∼1/7 of F_{ext} (Section 4-B). ΔF_{int} and F_{local} are conceptually equivalent to each other for crystalline ice. In accordance with these observations, previous theoretical calculations[30] suggest that the electric field variation due to the local field correction is typically <30% for frozen solvents.

6. SUMMARY

(i) We have studied the VSE of the hydroxyl stretch vibration of a crystalline ice sample under strong direct-current electric fields by monitoring the spectral changes of vibrationally decoupled O−H or O−D bands of dilute HOD in ice. This experiment measures the VSE induced only by an applied electrostatic field in the absence of other frequency-shifting effects such as those associated with structural changes of chromophore environment under the electric field.

DOI: 10.1021/acs.jpcc.5b01850
J. Phys. Chem. C 2015, 119, 15596−15603

(ii) The hydroxyl bands show discernible spectral broadening due to the VSE when the field strength exceeds ~1×10^7 V·m^{-1}. With increasing field strength, the spectral shape changes from a sharp Gaussian profile to a more broadened structure and then to a double-peak structure with a dip at the center. In addition, the spectral shape becomes slightly asymmetric under applied field.

(iii) The major features of the spectral changes appearing under the field can be reproduced by a numerical analysis model that calculates the integrated absorption of a collection of Stark-shifted oscillators in RAIRS geometry.

(iv) The Stark tuning rate of the hydroxyl stretch vibration is estimated to be $\Delta\mu$(O−D) = 6.4−12 cm^{-1}/(MV/cm) at $F = 1.8\times 10^8$ to 6.4×10^7 V·m^{-1} and $\Delta\mu$(O−H) = 10−16 cm^{-1}/(MV·cm^{-1}) at $F = 2.3 \times 10^8$ to 9.2×10^7 V·m^{-1}. The $\Delta\mu$ value is not constant in these field strength ranges. Instead, $\Delta\mu$ decreases with increasing field strength when it is deduced from eq 1, which assumes that $\Delta\mu$ is linear proportionality coefficient between $\Delta\nu$ and F. The isotopic effect on the Stark tuning rate is observed to be $\Delta\mu$(O−H)/$\Delta\mu$(O−D) = 1.5−1.8.

(v) The VSE of the hydroxyl stretch vibration of ice is uniquely large compared to the vibrations in other frozen molecular solids. The large $\Delta\mu$ value of ice can be attributed to its extensive hydrogen-bonding network. This interpretation is supported by quantum mechanical calculations of water cluster models, which illustrate that the intermolecular hydrogen bonding in water clusters increases the Stark shift of the hydroxyl stretch frequency.

■ ASSOCIATED CONTENT

Supporting Information

Numerical simulation of Stark-broadened RAIR spectra. The Supporting Information is available free of charge on the ACS Publications website at DOI: 10.1021/acs.jpcc.5b01850.

■ AUTHOR INFORMATION

Corresponding Authors

*E-mail: surfion@snu.ac.kr. Phone: +82-2-875-7471. (H.K.)
*E-mail: jinylee@skku.edu. (J.-Y.L.)

Notes

The authors declare no competing financial interest.

■ ACKNOWLEDGMENTS

We thank Prof. M. Yang (Chungbuk Univ.) for helpful discussions about theoretical modeling of VSE. This work was supported by Samsung Science and Technology Foundation (SSTF-BA1301-04).

■ REFERENCES

(1) Bublitz, G. U.; Boxer, S. G. Stark Spectroscopy: Applications in Chemistry, Biology, and Materials Science. *Annu. Rev. Phys. Chem.* **1997**, *48*, 213−242.

(2) Boxer, S. G. Stark Realities. *J. Phys. Chem. B* **2009**, *113*, 2972−2983.

(3) Corcelli, S. A.; Lawrence, C. P.; Skinner, J. L. Combined Electronic Structure/Molecular Dynamics Approach for Ultrafast Infrared Spectroscopy of Dilute HOD in Liquid H_2O and D_2O. *J. Chem. Phys.* **2004**, *120*, 8107−8117.

(4) Ham, S.; Kim, J.-H.; Lee, H.; Cho, M. Correlation Between Electronic and Molecular Structure Distortions and Vibrational Properties. II. Amide I Modes of NMA−nD_2O Complexes. *J. Chem. Phys.* **2003**, *118*, 3491−3498.

(5) Fried, S. D.; Bagchi, S.; Boxer, S. G. Measuring Electrostatic Fields in Both Hydrogen-Bonding and Non-Hydrogen-Bonding Environments Using Carbonyl Vibrational Probes. *J. Am. Chem. Soc.* **2013**, *135*, 11181−11192.

(6) Hermansson, K. Electric-Field Effects on the OH Vibrational Frequency and Infrared-Absorption Intensity for Water. *J. Chem. Phys.* **1993**, *99*, 861−868.

(7) Manca, C.; Allouche, A. Quantum Study of the Adsorption of Small Molecules on Ice: The Infrared Frequency of the Surface Hydroxyl Group and the Vibrational Stark Effect. *J. Chem. Phys.* **2001**, *114*, 4226−4234.

(8) Fried, S. D.; Wang, L.-P.; Boxer, S. G.; Ren, P.; Pande, V. S. Calculations of the Electric Fields in Liquid Solutions. *J. Phys. Chem. B* **2013**, *117*, 16236−16248.

(9) Zheng, J.; Kwak, K.; Fayer, M. Ultrafast 2D IR Vibrational Echo Spectroscopy. *Acc. Chem. Res.* **2007**, *40*, 75−83.

(10) Shi, L.; Gruenbaum, S. M.; Skinner, J. L. Interpretation of IR and Raman Line Shapes for H_2O and D_2O Ice Ih. *J. Phys. Chem. B* **2012**, *116*, 13821−13830.

(11) Haas, C.; Hornig, D. Inter-and Intramolecular Potentials and the Spectrum of Ice. *J. Chem. Phys.* **1960**, *32*, 1763−1769.

(12) Bertie, J. T.; Whalley, E. Infrared Spectra of Ices Ih and Ic in the Range 4000 to 350 cm^{-1}. *J. Chem. Phys.* **1964**, *40*, 1637−1645.

(13) Sivakumar, T.; Schuh, D.; Sceats, M. G.; Rice, S. A. The 2500−4000 cm^{-1} Raman and Infrared Spectra of Low Density Amorphous Solid Water and of Polycrystalline Ice I. *Chem. Phys. Lett.* **1977**, *48*, 212−218.

(14) Devlin, J. P.; Wooldridge, P. J.; Ritzhaupt, G. Decoupled Isotopomer Vibrational Frequencies in Cubic Ice: A Simple Unified View of the Fermi Diads of Decoupled H_2O, HOD, and D_2O. *J. Chem. Phys.* **1986**, *84*, 6095−6100.

(15) Perakis, F.; Widmer, S.; Hamm, P. Two-Dimensional Infrared Spectroscopy of Isotope-Diluted Ice Ih. *J. Chem. Phys.* **2011**, *134*, 204505.

(16) Shin, S.; Kim, Y.; Moon, E.-S.; Lee, D. H.; Kang, H.; Kang, H. Generation of Strong Electric Fields in an Ice Film Capacitor. *J. Chem. Phys.* **2013**, *139*, 074201.

(17) Shin, S.; Kim, Y.; Kang, H.; Kang, H. Effect of Electric Field on Condensed-Phase Molecular Systems. I. Dipolar Polarization of Amorphous Solid Acetone. *J. Phys. Chem. C* **2015**, DOI: 10.1021/acs.jpcc.5b01849.

(18) Haq, S.; Hodgson, A. Multilayer Growth and Wetting of Ru (0001). *J. Phys. Chem. C* **2007**, *111*, 5946−5953.

(19) Choi, J.-H.; Cho, M. Vibrational Solvatochromism and Electrochromism of Infrared Probe Molecules Containing C≡ O, C≡ N, C═ O, or C− F Vibrational Chromophore. *J. Chem. Phys.* **2011**, *134*, 154513.

(20) Saggu, M.; Levinson, N. M.; Boxer, S. G. Experimental Quantification of Electrostatics in X−H··· π Hydrogen Bonds. *J. Am. Chem. Soc.* **2012**, *134*, 18986−18997.

(21) Layfield, J. P.; Hammes-Schiffer, S. Calculation of Vibrational Shifts of Nitrile Probes in the Active Site of Ketosteroid Isomerase upon Ligand Binding. *J. Am. Chem. Soc.* **2013**, *135*, 717−725.

(22) Horowitz, Y.; Asscher, M. Low Energy Charged Particles Interacting with Amorphous Solid Water Layers. *J. Chem. Phys.* **2012**, *136*, 134701.

(23) Andrews, S. S.; Boxer, S. G. Vibrational Stark Effects of Nitriles I. Methods and Experimental Results. *J. Phys. Chem. A* **2000**, *104*, 11853−11863.

(24) Craig, D. P.; Thirunamachandran, T. *Molecular Quantum Electrodynamics: an Introduction to Radiation-Molecule Interactions;* Academic Press: London, 1984.

(25) Park, E. S.; Boxer, S. G. Origins of the Sensitivity of Molecular Vibrations to Electric Fields: Carbonyl and Nitrosyl Stretches in Model Compounds and Proteins. *J. Phys. Chem. B* **2002**, *106*, 5800−5806.

DOI: 10.1021/acs.jpcc.5b01850
J. Phys. Chem. C 2015, 119, 15596−15603

(26) Head-Gordon, M.; Pople, J. A.; Frisch, M. J. MP2 Energy Evaluation by Direct Methods. *Chem. Phys. Lett.* **1988**, *153*, 503−506.
(27) Frisch, M. J.; Head-Gordon, M.; Pople, J. A. A Direct MP2 Gradient Method. *Chem. Phys. Lett.* **1990**, *166*, 275−280.
(28) Frisch, M. J., et al. *Gaussian 09;* Gaussian, Inc.: Wallingford, CT, 2009.
(29) Corcelli, S. A.; Kelley, J. A.; Tully, J. C.; Johnson, M. A. Infrared Characterization of the Icosahedral Shell Closing in Cl-Center Dot H_2O Center Dot Ar-n ($1 \leq n \leq 13$) Clusters. *J. Phys. Chem. A* **2002**, *106*, 4872−4879.
(30) Bottcher, C. J. F. *Theory of Electric Polarization;* Elsevier Scientific Publishing Co: Amsterdam, New York, 1973.

DOI: 10.1021/acs.jpcc.5b01850
J. Phys. Chem. C 2015, 119, 15596−15603